Eur. Phys. J. C 24, 573–580 (2002)
Digital Object Identifier (DOI) 10.1007/s10052-002-0970-6

THE EUROPEAN
PHYSICAL JOURNAL C

Valence quark annihilation and leading charmed meson production in $\pi^- N$ and $K^- N$ collisions

T. Tashiro[1,a], H. Noda[2,b], K. Kinoshita[3,c], S. Nakariki[1]

[1] Department of Computer Simulation, Okayama University of Science, Okayama 700-0005, Japan
[2] Department of Mathematical Science, Ibaraki University, Mito 310-0056, Japan
[3] Physics Department, Kagoshima University, Kagoshima 890-0065, Japan

Received: 18 December 2001 / Revised version: 22 March 2002 /
Published online: 14 June 2002 –

Abstract. We discuss the hadroproduction of charmed mesons in the framework of the constituent cascade model taking into account the valence quark annihilation. It is shown that the valence quark annihilation process dominates at large Feynman x regions and explains the recent experimental data on the asymmetry between D^0 and $\bar{D}^0$ at 350 GeV/c in $\pi^- N$ collisions.

1 Introduction

Perturbative QCD based on the factorization theorem provides a reasonable description of experimental data on the inclusive cross sections of heavy quark production [1,2], however, there are uncertainties in the formalism as reviewed in [3,4]. The perturbative calculations of cross sections of charmed particles are sensitive to the parameters of the renormalization and factorization scales, and the shape of differential cross sections of D mesons are quite similar to the next to leading order (NLO) QCD predictions for c quark hadroproduction without the intrinsic transverse momentum and the fragmentation function [3, 5]. The azimuthal correlations of two heavy quarks are not reproduced satisfactorily without intrinsic transverse momenta of incident partons [3,4,6]. Though the resummation of large logarithmic terms improves the description of heavy quark production, it is still insufficient to describe the spectra both in the central and the forward regions [7]. Although there are attempts to use the fragmentation function on calculating the perturbative approach [8,9], hadronization of heavy quarks is still an open problem, since it is an intrinsically non-perturbative process.

Recently, experiments at CERN [10] measured the neutral D mesons in π^- nucleus collisions and observed much smaller values for the leading/non-leading asymmetry than those of charged D mesons i.e. less than 0.2 and even a negative value around $x \approx 0.8$. The experimental data on the asymmetry of charged D mesons increases from zero to nearly one with Feynman variable x in the π^- fragmentation region [10,11]. The leading particle contains the same type of quark as one of the valence quarks in the incident hadron, while the non-leading one does not contain the projectile valence quarks. For example, the asymmetry of $D^0(c\bar{u})/\bar{D}^0(u\bar{c})$ in a $\pi^-(d\bar{u})$ interaction with a nucleon is defined as

$$A_{\pi^- N}(D^0, \bar{D}^0) = \frac{\sigma(D^0) - \sigma(\bar{D}^0)}{\sigma(D^0) + \sigma(\bar{D}^0)}. \tag{1}$$

In the perturbative QCD at leading order, the factorization theorem predicts that c and $\bar{c}$ quarks are produced with the same distributions and then fragment independently. In this case the asymmetry $A_{\pi^- N}(D^-, D^+)$ is equal to zero. Even in the case of NLO QCD, the predicted asymmetry is much smaller than the data [12,13]. The asymmetry $A_{\pi^- N}(D^-, D^+)$ has been investigated and explained by means of many approaches: string fragmentation [14], intrinsic charm contributions [15,16], recombination processes [17–20], recombination using the valon concept [21], light quark fragmentation [22] and so on. Production asymmetries between charm and anticharm mesons are also observed in photoproduction experiments [23]. Recently, a perturbative recombination mechanism was proposed and applied to the charmed meson asymmetry observed in photoproduction experiments successfully [24]. Although several models have been applied more or less satisfactorily to $A_{\pi^- p}(D^0, \bar{D}^0)$ at $x \lesssim 0.6$ [16,19], the asymmetry problem of the charmed hadron productions is an open question.

We have proposed the constituent quark–diquark cascade model and explained the leading/non-leading asymmetry of charged D mesons $A_{\pi^- N}(D^-, D^+)$ successfully [25]. The model, however, gives rather large values of $A_{\pi^- N}(D^0, \bar{D}^0)$ at $0.5 \lesssim x$ as expected from the leading particle effect but deviating from the experimental data.

In the present paper, we investigate the leading/non-leading D meson asymmetry in the framework of the con-

[a] e-mail: tashiro@sp.ous.ac.jp, nakariki@sp.ous.ac.jp
[b] e-mail: noda@mito.ipc.ibaraki.ac.jp
[c] e-mail: kisei@edu.kagoshima-u.ac.jp

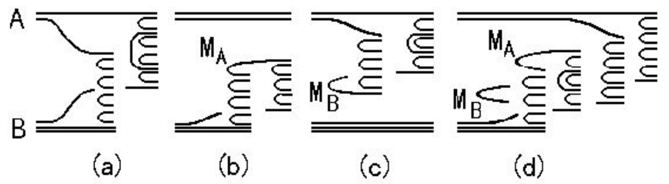

Fig. 1a–d. The interaction mechanism in AB collision: **a** non-diffractive dissociation type, **b**, **c** single-diffractive and **d** double-diffractive dissociation type mechanisms

stituent quark–diquark cascade model by taking into account the valence quark annihilation. We show that the valence quark annihilation process dominates at large Feynman x regions and explains the recent experimental data on the asymmetry between D^0 and $\bar{D}^0$ at 350 GeV/c in $\pi^- N$ collisions. Also, we show the prediction of asymmetries between D and $\bar{D}$ in $K^- N$ collision.

2 Constituent cascade model with valence quark annihilation mechanism

2.1 Framework of the model

We briefly review the previous model [25] and then introduce the valence quark annihilation mechanism into the model. We consider an inclusive reaction $A + B \to C + X$ in the centre of mass system of A and B. The light-like variables of A and B are defined as follows:

$$x_{0\pm}^A = \frac{E^A \pm p_{\rm cm}}{\sqrt{s_0}}, \quad x_{0\pm}^B = \frac{E^B \mp p_{\rm cm}}{\sqrt{s_0}}, \tag{2}$$

where $s_0^{1/2}$ is the centre of mass energy of the incident hadrons A and B.

When the collision between A and B occurs, the incident hadrons break up into two constituents with a probability $(1 - P_{\rm gl})$; otherwise they emit gluons with $P_{\rm gl}$ followed by a quark–antiquark pair creation. We assume four interaction types: (a) non-diffractive dissociation, (b) and (c) single-diffractive dissociations of B and A, and (d) double-diffractive dissociation, as shown in Fig. 1. The probabilities of these types to occur are $(1-P_{\rm gl})^2$, $P_{\rm gl}(1-P_{\rm gl})$, $P_{\rm gl}(1 - P_{\rm gl})$ and $P_{\rm gl}^2$, respectively. Here we denote the quark–antiquark pair emitted from A (B) via the gluons as M_A (M_B). The probabilities of M_A (M_B) to be $u\bar{u}, d\bar{d}, s\bar{s}$ and $c\bar{c}$ are denoted $P_{u\bar{u}}$, $P_{d\bar{d}}$, $P_{s\bar{s}}$ and $P_{c\bar{c}}$, respectively. The momentum fraction of M_A is fixed by the distribution function

$$H_{M_A/A}(z) = z^{\beta_{\rm gl}-1}(1-z)^{\beta_{\rm ld}-1}/B(\beta_{\rm gl}, \beta_{\rm ld}), \tag{3}$$

and the uniform distribution R in the interval from zero to one as

$$x_+^{M_A} = x_{0+}^A z, \quad x_-^{M_A} = x_{0-}^A R. \tag{4}$$

Then the incident particles A and B have the following momentum fractions:

$$x_+^A = x_{0+}^A(1-z), \; x_-^A = m_A^2/(x_+^A \; s_0),$$

$$x_-^B = x_{0-}^B - (x_-^A - x_{0-}^A(1-R)), \; x_+^B = x_{0+}^B, \tag{5}$$

where the mass shell condition is considered and transverse momenta are neglected. The momentum fraction of M_B is treated similarly, exchanging the role of A and B.

In the centre of mass system of incidents $A(M_A)$ and $B(M_B)$, we define the light-like fractions of these hadrons and fix the light-like fractions of the projectile constituents. The distribution functions of the constituents in the projectile A composed of a and a' are described by

$$H_{a/A}(z) = H_{a'/A}(1-z) = \frac{z^{\beta_a - 1}(1-z)^{\beta_{a'}-1}}{B(\beta_a, \beta_{a'})}. \tag{6}$$

Then the light-like fractions of a and a' are

$$x_+^a = x_{0+}^A z, \quad x_-^a = x_{0-}^A R, \quad x_+^{a'} = x_{0+}^A - x_+^a$$

and

$$x_-^{a'} = x_{0-}^A - x_-^a,$$

where $x_{0\pm}^A$ are the light-like fractions of the projectile A defined in the centre of mass system of the incidents A and $B(M_B)$. The distribution functions of the constituents in M_A, B and M_B are similarly defined.

In this model hadrons are produced on the chain between a valence quark (antiquark) from $A(M_A)$ and the valence diquark (quark) from $B(M_B)$. The small intrinsic transverse momenta of constituents are introduced by changing the direction of the incident constituents by an angle $\varphi_{\rm in}$ in the rest frame of the chain. Here we choose the distributions for $z = \cos\varphi_{\rm in}$ as

$$D_{\rm in}(z) = \frac{\beta_{\rm in}+1}{2^{\beta_{\rm in}+1}}(1+z)^{\beta_{\rm in}} \tag{7}$$

in the region $-1 < z < 1$. Hadrons are produced by the cascade processes

$$\begin{aligned} q &\to M(q\bar{q}') + q', \\ &\quad B(q[q'q'']) + \overline{[q'q'']}, B(q\{q'q''\}) + \overline{\{q'q''\}}, \\ \overline{[q'q'']} &\to \overline{B}(\bar{q}\overline{[q'q'']}) + q, \\ &\quad M(q\bar{q}') + \overline{[qq'']}, M(q\bar{q}') + \overline{\{qq''\}}, \\ \overline{\{q'q''\}} &\to \overline{B}(\bar{q}\overline{\{q'q''\}}) + q, \\ &\quad M(q\bar{q}') + \overline{[qq'']}, M(q\bar{q}') + \overline{\{qq''\}}, \end{aligned} \tag{8}$$

where q denotes u, d, s and c and $[q'q'']$ denotes $[ud], [us]$, $[uc]$, $[ds], [dc]$ and $[sc]$ and so on. The symbols [ ] and {} denote the flavour antisymmetric and symmetric diquarks, respectively. Meson production probabilities from $q, \overline{[q'q'']}$ and $\overline{\{q'q''\}}$ are $1-\epsilon, \eta_{[]}$ and $\eta_{\{\}}$, respectively. The pair creation probabilities $P_{u\bar{u}}$, $P_{d\bar{d}}$, $P_{s\bar{s}}$ and $P_{c\bar{c}}$ are also assumed in the cascade process. The probabilities of $[qq']\overline{[qq']}$, $\{qq'\}\overline{\{qq'\}}$ and $\{qq\}\overline{\{qq\}}$ pair creations from a quark are chosen as $\epsilon P_{q\bar{q}} P_{q'\bar{q}'}, \epsilon P_{q\bar{q}} P_{q'\bar{q}'}$ and $\epsilon {P_{q\bar{q}}}^2$, respectively.

For the cascade process $a \to H(a\bar{b}) + b$ on the beam (target) side, the distribution function of the light-like fraction of b, x_+^b (x_-^b), is assumed to be

$$F_{ba}(z) = z^{\gamma\beta_a - 1}(1-z)^{\beta_a + \beta_b - 1}/B(\gamma\beta_a, \beta_a + \beta_b). \tag{9}$$

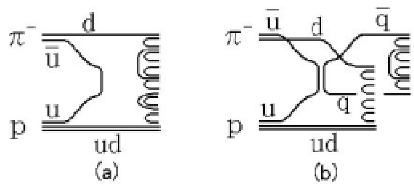

Fig. 2a,b. The valence quark annihilation processes in $\pi^- p$ collision

Furthermore, the transverse momentum distribution of H is phenomenologically assumed to be the following function:

$$G(\boldsymbol{p}_{\mathrm{T}}^2) = \frac{\sqrt{m_H}}{C} \exp\left(-\frac{C}{\sqrt{m_H}}\boldsymbol{p}_{\mathrm{T}}^2\right) \tag{10}$$

in $\boldsymbol{p}_{\mathrm{T}}^2$ space, where m_H denotes the mass of H. The parameter C is fixed by the experimental data on the $\boldsymbol{p}_{\mathrm{T}}^2$ distributions. The dynamical parameters β in (6) and (9), which determine the momentum sharings of the constituents, are related to the intercepts of the Regge trajectories by $\beta_u = \beta_d = 1-\alpha_{\rho-\omega}(0)$, $\beta_s = 1-\alpha_\phi(0)$, $\beta_c = 1-\alpha_{J/\psi}(0)$ [26,27]. From previous analyses [28,29], we determine the values for diquarks as $\beta_{[ij]} = \gamma_{[]}(\beta_i+\beta_j)$, $\beta_{\{ij\}} = \gamma_{\{\}}(\beta_i+\beta_j)$.

We now see how the cascade processes occurs between the incident constituents, for example, q from A (M_A) and $\{q'q''\}$ from B. We redefine the light-like fractions of q and $\{q'q''\}$ in their rest frame. The momentum sharing of the cascade process $q+\{q'q''\} \to H(q\bar{b}) + b + \{q'q''\}$ from q with $x_\pm^q$ and $\{q'q''\}$ with $x_\pm^{\{q'q''\}}$ takes place as follows [29, 30]: using (9) with $a=q$, we fix the light-like fraction of b and $H(q\bar{b})$ as $x_+^b = x_+^q z$ and $x_+^H = x_+^q - x_+^b$, respectively and put $x_-^b = x_-^q$. The transverse momentum of H is fixed by (10). Then x_-^H is fixed from the on shell condition $x_+^H x_-^H = (m_H^2+\boldsymbol{p}_{\mathrm{T}}^2)/s'$, where $s'^{1/2}$ is the subenergy of the incident q and $\{q'q''\}$ system. The transverse momentum of b is $\boldsymbol{p}_{\mathrm{T}}^b = \boldsymbol{p}_{\mathrm{T}}^q - \boldsymbol{p}_{\mathrm{T}}^H$. The light-like fraction of $\{q'q''\}$ is decreased to $\tilde{x}_-^{\{q'q''\}} = x_-^{\{q'q''\}} - x_-^H$. If the energy of the $b+\{q'q''\}$ system is enough to create another hadron, a cascade such as $b+\{q'q''\} \to b + H(c\{q'q''\}) + \bar{c}$ takes place on the opposite side. In the final step, we assume that the constituents recombine into one or two hadrons according to the processes: $q+\bar{q}' \to M(q\bar{q}')$, $q+[q'q''] \to B(q[q'q''])$, $\{qq'\} + \overline{[q''q''']} \to M(q\overline{q''}) + M(q'\overline{q'''})$ and so on. The momenta of the recombined hadrons are the sum of those of the final constituents and are off shell. In the cms of incident hadrons A and B, we have $\sum_i \boldsymbol{p}_i = 0$ and $\sum_i p_i^0 = s_0^{1/2}$, where $\boldsymbol{p}_i$ denotes the three momentum of the ith produced particle. In order to put recombined hadrons on shell, we multiply the three momenta of all produced hadrons by a common factor α so that the summation $\sum_i((\alpha\boldsymbol{p}_i)^2+m_i^2)^{1/2}$ would be equal to $s_0^{1/2}$ as explained in [25].

The effect of scalar and axial vector meson productions on D mesons are small as compared with pseudoscalar (PS), vector (V) and tensor (T) mesons in the energy

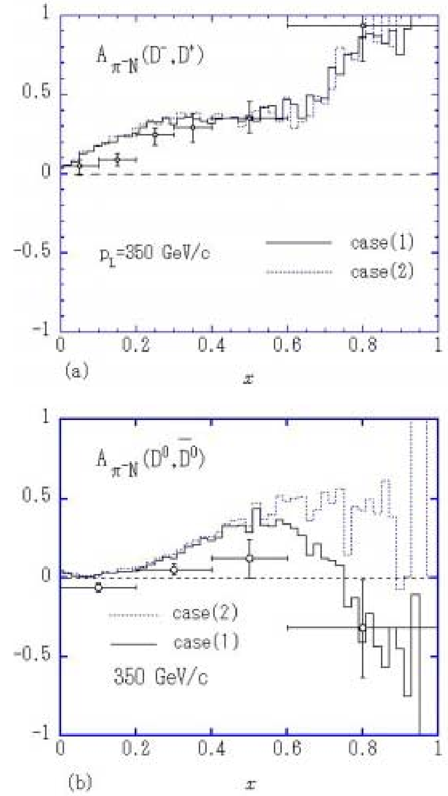

Fig. 3a,b. The x-dependences of asymmetries **a** $A_{\pi^-N}(D^-, D^+)$ and **b** $A_{\pi^-N}(D^0,\bar{D}^0)$ at $p_{\mathrm{L}} = 350\,\mathrm{GeV}/c$. The full lines show the results in case (1) and the dotted lines in case (2). The experimental data are taken from [10]

region under consideration. Therefore we only take account of PS, V and T mesons. The production probabilities for them are assumed to be P_{PS}, P_V and P_{T} ($P_T = 1 - P_{PS} - P_V$). For baryons we consider lower lying baryons: octet (B_8) and decuplet (B_{10}) baryons composed of u, d, and s flavours and the corresponding hadrons with charm flavour. Octet and decuplet baryons are described by

$$|B_8\rangle = \cos\theta|q[q'q'']\rangle + \sin\theta|q\{q'q''\}\rangle, \tag{11}$$
$$|B_{10}\rangle = |q\{q'q''\}\rangle. \tag{12}$$

We assume the production probabilities for them to be P_{B8} and P_{B10} ($P_{B10} = 1 - P_{B8}$), respectively. Then the emission probabilities of individual cascade processes are determined by the above probabilities. For examples, the probabilities to produce $\pi^+, \rho^+, a_2^+, ..., \Delta^{++}, p, \Delta^+, ...,$ Ξ_{cc}^{++} and Ξ_{cc}^{*++} from a u quark are as follows:

$$(1-\epsilon)P_{d\bar{d}}P_{PS}, \quad (1-\epsilon)P_{d\bar{d}}P_V, \quad (1-\epsilon)P_{d\bar{d}}P_T, ...,$$
$$\epsilon P_{u\bar{u}}^{\,2}, \quad \epsilon P_{u\bar{u}}P_{d\bar{d}}\frac{1}{3}P_{B8}\sin^2\theta \Big/ \left(\frac{1}{3}P_{B8}\sin^2\theta + \frac{2}{3}P_{B10}\right),$$
$$\epsilon P_{u\bar{u}}P_{d\bar{d}}\frac{2}{3}P_{B10} \Big/ \left(\frac{1}{3}P_{B8}\sin^2\theta + \frac{2}{3}P_{B10}\right), ...,$$
$$\epsilon P_{c\bar{c}}^{\,2}\frac{2}{3}P_{B8}\sin^2\theta \Big/ \left(\frac{2}{3}P_{B8}\sin^2\theta + \frac{1}{3}P_{B10}\right),$$

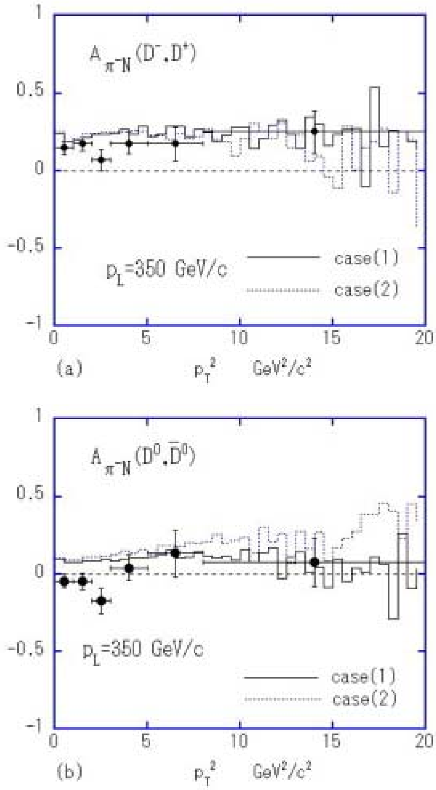

Fig. 4a,b. The p_{T}^2-dependences of asymmetries **a** $A_{\pi^- N}(D^-, D^+)$ and **b** $A_{\pi^- N}(D^0, \bar{D}^0)$ at $p_{\mathrm{L}} = 350\,\mathrm{GeV}/c$. The full lines show the results in case (1) and the dotted lines in case (2). The experimental data are taken from [10]

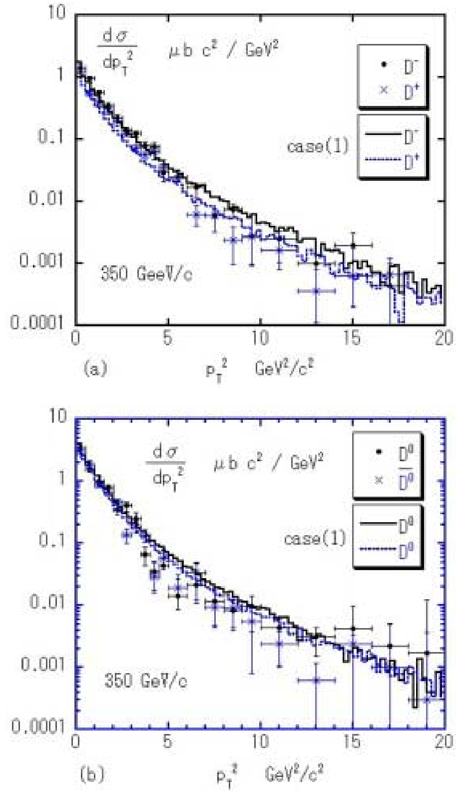

Fig. 5a,b. The p_{T}^2-dependences in the range $0 \le x \le 1$ of **a** $D^{\pm}$ and **b** D^0 and $\bar{D}^0$ mesons at $P_{\mathrm{L}} = 350\,\mathrm{GeV}/c$ for case (1) with valence quark annihilation. The experimental data are taken from [10]

$$\epsilon P_{c\bar{c}}{}^2 \frac{1}{3} P_{B10} \Big/ \left(\frac{2}{3} P_{B8} \sin^2\theta + \frac{1}{3} P_{B10} \right),$$

where the factors 1/3 and 1/2 are flavour $SU(4)$ factors. Directly produced resonances decay into stable particles. Details of our model are explained in [25,28,29].

2.2 Valence quark annihilation mechanism

In order to explain the x distribution of $A_{\pi^- p}(D^0, \bar{D}^0)$, we introduce the valence quark annihilation process into the previous model [25]. Let us consider the case of a $\pi^- p$ collision. We take account of the annihilation of the valence $\bar{u}$ from π^- and valence u from the proton target in a way slightly different from the one pointed out in [17,19]. There are annihilation processes such as shown in Fig. 2a,b. The annihilation process in Fig. 2a is considered a soft process and its contribution is related to the magnitude of $\sigma_{\mathrm{inel}}^{\pi^-} - \sigma_{\mathrm{inel}}^{\pi^+}$ by unitarity. This process, however, may be negligible for the charm-pair production. Here we only consider the annihilation process in Fig. 2b. Here we assume that the process

$$\bar{u} + u \to \bar{q} + q \to \text{“hadrons”} + \text{“hadrons”} \tag{13}$$

occurs with the probability P_{an} and the non-annihilation type occurs with the probability $1 - P_{\mathrm{an}}$. Branching ratios of $\bar{u}u \to \bar{u}u, \bar{d}d, \bar{s}s$, and $\bar{c}c$ are chosen to be equal to $P_{u\bar{u}}, P_{d\bar{d}}, P_{s\bar{s}}$ and $P_{c\bar{c}}$ for the channels allowed energetically. The produced $\bar{q}$ and q in (13) are supposed to be non-free in terms of the hadronization mechanism. Thus it is assumed that $\bar{q}$ has a tendency to be produced in the forward direction of $\bar{u}$ in the π^- beam. Here we choose the distributions for $z = \cos\varphi_{\mathrm{an}}$ as

$$D_{\mathrm{an}}(z) = \frac{\beta_{\mathrm{an}} + 1}{2^{\beta_{\mathrm{an}}+1}} (1+z)^{\beta_{\mathrm{an}}} \tag{14}$$

in the region $-1 < z < 1$, where φ_{an} is the angle between the directions of $\bar{u}$ and $\bar{q}$. We use a smaller value of β_{an} as compared with β_{in} in (7). After the annihilation process, the non-diffractive type production of hadrons occurs as shown in Fig. 2b. The effect of the annihilation processes $\bar{u}u \to \bar{u}u, \bar{d}d$, and $\bar{s}s$ on light hadron productions is very small and does not affect the light hadron spectra. When the incident constituents in (M_A and B), (A and M_B) or (M_A and M_B) are quark and its antiquark, it is assumed that the annihilation process also occurs with the same probability P_{an} for the interaction types in Figs. 1b–d.

3 Comparison with the data

In this section, we give the results of our model for the inclusive hadron productions in $\pi^- N$ collisions. The probability of the incident hadron to emit gluons followed by

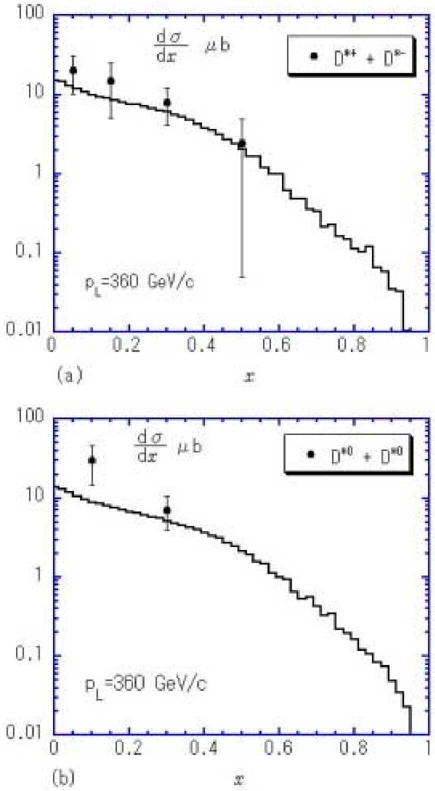

Fig. 6a,b. Comparison of the model with the experimental data on the x-dependences for productions of **a** D^{*+} or D^{*-} and **b** D^{*0} or $\bar{D}^{*0}$ mesons at $P_{\rm L} = 360\,{\rm GeV}/c$ [32]. The theoretical lines were calculated for $P_{\rm L} = 350\,{\rm GeV}/c$, the full line is for case (1) with the valence quark annihilation

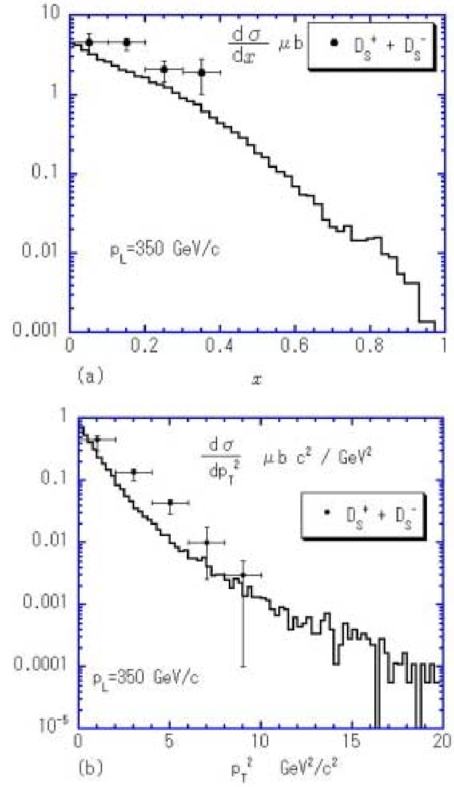

Fig. 7a,b. Differential cross sections with respect to **a** x and **b** $p_{\rm T}^2$ for production of D_S^+ or D_S^- at $P_{\rm L} = 350\,{\rm GeV}/c$. The full line denotes the results for case (1). The experimental data are taken from [10]

a quark–antiquark pair is chosen as $P_{\rm gl} = 0.15$ and the parameters in (3) as $\beta_{\rm gl} = 0.44$, $\beta_{\rm ld} = 1.0$. Meson production probabilities from $q, \overline{[q'q'']}, \overline{\{q'q''\}}$ in (8) are chosen as $(1-\epsilon) = 0.93$, $\eta_{[]} = \eta_{\{\}} = 0.25$. The parameter of the intrinsic $p_{\rm T}$ distributions of the constituents in (3) is chosen as $\beta_{\rm in} = 40$. The values of the dynamical parameters of the momentum sharing function in (9) are fixed by the intercepts of the ρ and ϕ trajectories as $\beta_u = \beta_d = 0.5$, $\beta_s = 1.0$ and $\gamma = 1.75$. The parameter for the c quark is chosen as $\beta_c = 4.0$. This is in accord with the argument that the slopes of Regge trajectories of charmed mesons are smaller than those of light mesons as discussed in [31]. The dynamical parameters of the momentum sharing for symmetric and antisymmetric diquarks are assumed to be $\gamma_{\{\}} = 2.0, \gamma_{[]} = 1.5$. The parameter of the $p_{\rm T}^2$ distribution is chosen as $C = 1.8$ and the probabilities are $P_{u\bar{u}} = P_{d\bar{d}} = 0.435$, $P_{s\bar{s}} = 0.1297$ and $P_{c\bar{c}} = 1 - 2P_{u\bar{u}} - P_{s\bar{s}} = 0.0003$. Furthermore the meson production probabilities are assumed to be $P_{PS} = 1/9, P_V = 3/9$ and $P_T = 5/9$ for mesons. We put the parameter $P_{\rm an}$ so as to reproduce the asymmetry $A_{\pi^-N}(D^0, \bar{D}^0)$. We choose the value $P_{\rm an} = 0.2$. This value scarcely changes the features of the spectra of light hadrons composed of u, d and s quarks. The parameter of the $p_{\rm T}$ distributions of $\bar{q}$ and q in valence quark annihilation in (13) is chosen as $\beta_{\rm an} = 20$ in (14).

In Fig. 3 the results of the x-dependence of $A_{\pi^-N}(D^-, D^+)$ and $A_{\pi^-N}(D^0, \bar{D}^0)$ are compared with the experimental data at $350\,{\rm GeV}/c$ [10] and compare the two cases, case (1) with the valence quark annihilation and case (2) without the valence quark annihilation. The model of case (1) is in good agreement with the experimental data. The negative value of $A_{\pi^-N}(D^0, \bar{D}^0)$ at large x is well explained by introducing a small amount of the valence quark annihilation process to the model. We compare our calculations with the $p_{\rm T}^2$- dependences of asymmetries $A_{\pi^-N}(D^-, D^+)$ and $A_{\pi^-N}(D^0, \bar{D}^0)$ in Fig. 4. Our model gives small positive values and is in qualitative agreement with the data at $p_{\rm T}^2 \gtrsim 4\,({\rm GeV}/c)^2$. In Fig. 5, we show the results of the $p_{\rm T}^2$-dependence of D mesons in $\pi^- N$ collisions for case (1). The newly introduced annihilation process explains the large $p_{\rm T}^2$ charmed meson productions in part. Our model is in good agreement with the data.

In Fig. 6 we show the results of D^* productions and compare the model of case (1). Our model gives a satisfactory description of the x-dependences for production of $D^{*+} + D^{*-}$ in $\pi^- N$ collisions. The slope of $D^{*0} + \bar{D}^{*0}$ production is somewhat small as compared with the experimental data [32].

The results of the x- and $p_{\rm T}^2$-dependences for production of $D_S^-(s\bar{c})$ or $D_S^+(c\bar{s})$ by the model of case (1) are compared with the experimental data [10] in Fig. 7. The features of the spectra are in good agreement with the

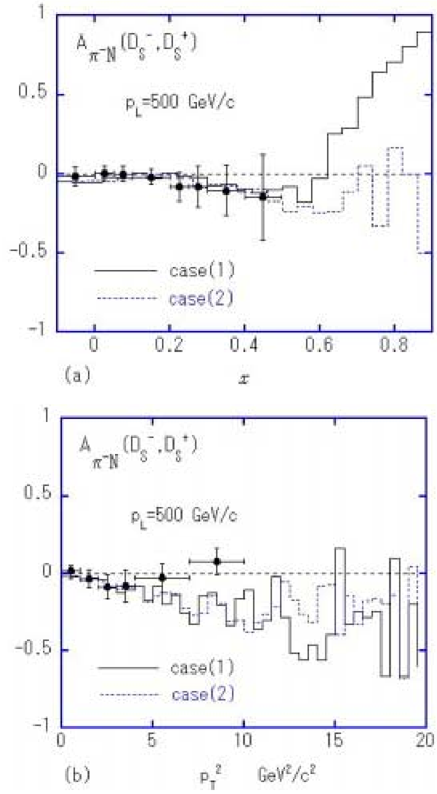

Fig. 8a,b. Asymmetries $A_{\pi^- N}(D_S^-, D_S^+)$ with respect to **a** x in the range $0 < p_T^2 < 10\,\mathrm{GeV}^2/c^2$ and **b** p_T^2 in the range $-0.1 < x < 0.5$ at $P_L = 500\,\mathrm{GeV}/c$. The full line denotes the results for case (1). The experimental data are taken from [33]

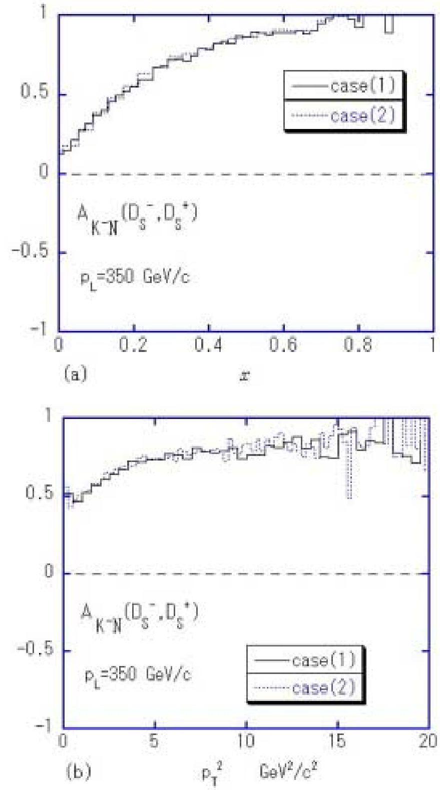

Fig. 9a,b. Asymmetries $A_{K^- N}(D_S^-, D_S^+)$ with respect to **a** x and **b** p_T^2 at $P_L = 350\,\mathrm{GeV}/c$. The full lines show the results in case (1) and the dotted lines in case (2)

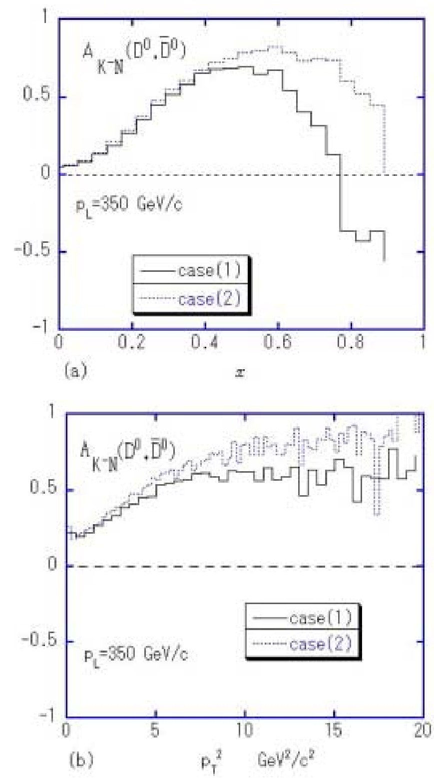

Fig. 10a,b. Asymmetries $A_{K^- N}(D^0, \bar{D}^0)$ with respect to **a** x and **b** p_T^2 at $P_L = 350\,\mathrm{GeV}/c$. The full lines show the results in case (1) and the dotted lines in case (2)

data except for the small discrepancy in normalization. In Fig. 8 we plot the experimental data on the asymmetries $A_{\pi^- N}(D_S^-, D_S^+)$ with respect to x and p_T^2 at $p_L = 500\,\mathrm{GeV}/c$ [33] together with the model predictions. The values are small because both $D_S^\pm$ mesons are non-leading particles. But $A_{\pi^- N}(D_S^-, D_S^+)$ increases with x at large x due to the valence quark annihilation. The model agrees with the experimental data on the x distribution but disagrees with the data on the p_T^2 distribution at $p_T^2 \gtrsim 5\,(\mathrm{GeV}/c)^2$.

We now turn to predictions of charmed mesons in $K^- N$ collisions and show the results at $p_L = 350\,\mathrm{GeV}/c$ in Figs. 9–11. The incident valence s quark is harder than $\bar{u}$ in the K^- beam. This results in strong asymmetries $A_{K^- N}(D_S^-, D_S^+)$ and $A_{K^- N}(D^0, \bar{D}^0)$ both for x- and p_T^2-dependences as shown in Figs. 9 and 10. The annihilation effects on the x- and p_T^2-dependences of $A_{K^- N}(D^0, \bar{D}^0)$ are large as shown in Fig. 10. It is noted that our model predicts large negative values of $A_{K^- N}(D^-, D^+)$ both for x- and p_T^2-dependences, though D^- and D^+ are non-leading particles. To illustrate this, we take account of only the non-diffractive type (Fig. 1a), which is the main part of hadron production. We consider the lowest cascade steps to produce $D^\pm$ mesons from the incident valence quarks s and $\bar{u}$:

$$s \to D_S^- + c \to D_S^- + D^+ + d, \qquad (15a)$$

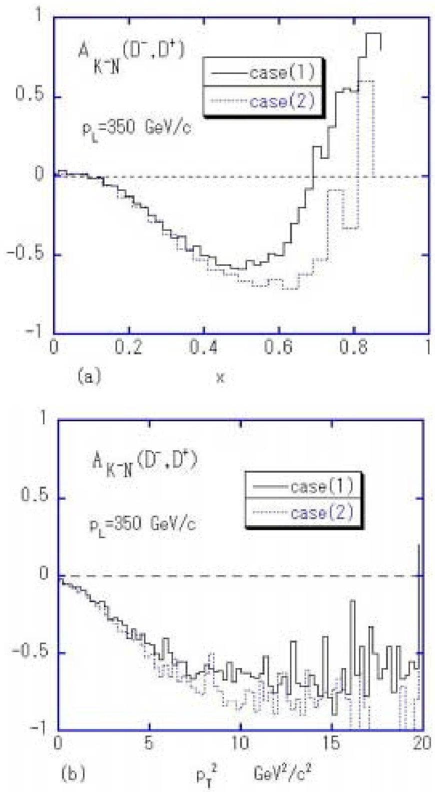

Fig. 11a,b. Asymmetries $A_{K^-N}(D^-, D^+)$ with respect to **a** x and **b** p_T^2 at $P_L = 350\,\mathrm{GeV}/c$. The full lines show the results in case (1) and the dotted lines in case (2)

$$s \to \bar{K}^0 + d \to \bar{K}^0 + D^- + c, \tag{15b}$$

$$\bar{u} \to D^0 + \bar{c} \to D^0 + D^- + \bar{d}, \tag{16a}$$

$$\bar{u} \to \pi^- + \bar{d} \to \pi^- + D^+ + \bar{c}. \tag{16b}$$

The valence s quark (15) is harder than the valence $\bar{u}$ quark (16). The distribution function (9) of the produced c quark in (15a) is harder than that of the d quark in (15b). Consequently, the single particle distribution of D^+ in (15a) is higher than that of D^- in (15b) at large x. The production ratio of D^+ in (15a) to D^- in (16a) behaves as $(1-x)^{\beta_s - \beta_u} = (1-x)^{0.5}$ at $x \sim 1$ due to the distribution function (9). Therefore the asymmetry $A_{K^-N}(D^-, D^+)$ has an appreciable negative value at intermediate x and increases with x at $x \sim 1$ even in the case (2).

4 Conclusions

(1) The large leading/non-leading asymmetry $A_{\pi^-N}(D^-, D^+)$ is naturally explained by our constituent quark cascade model as in the case of hadron productions composed of light quarks. The annihilation effect is small because we assumed that the produced $\bar{c}$ quark maintains the direction of the incident $\bar{u}$ quark in π^- beam.
(2) Only the resonance decay $D^{*-} \to \bar{D}^0 + \pi^-$ cannot explain the small and negative value of $A_{\pi^-N}(D^0, \bar{D}^0)$ observed in the recent experiment [10]. The valence quark annihilation process (13) explains the negative value of $A_{\pi^-N}(D^0, \bar{D}^0)$ at large x. Our model can explain the spectra up to the region $p_T^2 \lesssim 10\,(\mathrm{GeV}/c)^2$. It is interesting to apply the perturbative recombination mechanism [24] to the asymmetries $A_{\pi^-p}(D^0, \bar{D}^0)$ and $A_{\pi^-N}(D^-, D^+)$, and to see the recombination effect of the c quark with the incident antiquarks and annihilation effect.
(3) The model reproduces the small asymmetry $A_{\pi^-N}(D_S^-, D_S^+)$ at $x \lesssim 0.5$ as well as the strong asymmetry at large x due to the annihilation effect in case (1). This is because the created $\bar{c}$ quark in (13) is assumed to maintain the direction of incident π^- beam by the colour force between the $\bar{c}$ and the incident d quark. The result of the p_T^2-dependence shows a discrepancy at $5\,\mathrm{GeV}^2/c^2 < p_T^2$.
(4) Our model predicts strong asymmetries $A_{K^-N}(D_S^-, D_S^+)$ and $A_{K^-N}(D^0, \bar{D}^0)$ both for the x- and p_T^2-dependences as compared with those in π^- interactions. Our calculation shows large negative values of $A_{K^-N}(D^-, D^+)$ both for x- and p_T^2-dependences.

It is important to investigate the leading/non-leading asymmetries of charmed baryons in π^-N and K^-N and charmed hadrons in Σ^-N collisions. There are annihilation processes in $\pi^\pm N$ and K^-N and there is no annihilation process in K^+N and Σ^-N collisions. These points will be discussed elsewhere.

Acknowledgements. This work was supported by grant of the Academic Frontier Project promoted by the Ministry of Education, Culture, Sports, Science and Technology, Japan.

References

1. P. Nason, S. Dawson, K. Ellis, Nucl. Phys. B **303**, 607 (1988); G. Altarelli, M. Diemoz, G. Martinelli, P. Nason, Nucl. Phys. B **308**, 724 (1988); J.C. Collins, D.E. Soper, G. Sterman, Nucl. Phys. B **308**, 833 (1988); J. Qiu, G. Sterman, Nucl. Phys. B **353**, 105 (1991); B **353**, 137 (1991); W. Beenakker, H. Kuijf, W.L. Van Neerven, J. Smith, Phys. Rev. D **40**, 54 (1989)
2. M.L. Mangano, P. Nason, G. Ridolfi, Nucl. Phys. B **373**, 295 (1992); B **405**, 507 (1993)
3. S. Frixione, M.L. Mangano, P. Nason, G. Ridolfi, Adv. Ser. Direct in High Energy Phys. **15**, 609 (1998) [hep-ph/9702287]
4. J.C. Anjos, E. Cuautle, hep-ph/0005057
5. G.A. Alves et al. (E769), Phys. Rev. Lett. **77**, 2388 (1996); **77**, 2392 (1996)
6. M.G. Ryskin, A.G. Shuvaev, Yu.M. Shabelski, Phys. Atom. Nucl. **64**, 120 (2001); **64**, 1995 (2001); M.G. Ryskin, Yu.M. Shabelski, A.G. Shuvaev, hep-ph/0011111
7. M. Cacciari, M. Greco, Nucl. Phys. B **421**, 530 (1994); F.I. Olness, R.J. Scalise, W. Tung, Phys. Rev. D **59**, 014506 (1999); R.D. Ball, R.K. Ellis, JHEP **0105**, 053 (2001)
8. M. Cacciari, M. Greco, S. Rolli, A. Tanzini, Phys. Rev. D **55**, 2736 (1997)
9. E. Braaten, Yu Jia, T. Mehen, hep-ph/0108201
10. M. Adamovich et al. (WA92), Nucl. Phys. B **495**, 3 (1997)
11. M. Adamovich et al. (WA82), Phys. Lett. B **305**, 402 (1993); G.A. Alves et al. (E769), Phys. Rev. Lett. **72**, 812

(1994); E.M. Aitala et al. (E791), Phys. Lett. B **371**, 157 (1996)
12. P. Nason, S. Dawson, K. Ellis, Nucl. Phys. B **327**, 49 (1989); W. Beenakker, R. Meng, G.A. Schulter, J. Smith, W.L. Van Neerven, Nucl. Phys. B **351**, 507 (1991)
13. S. Frixione, M.L. Mangano, P. Nason, G. Ridolfi, Nucl. Phys. B **431**, 453 (1994)
14. H.U. Bengtsson, T. Sjöstrand, Comput. Phys. Commun. **46**, 43 (1987); E. Norrbin, T. Sjöstrand, Phys. Lett. B **442**, 407 (1998)
15. R. Vogt, S.J. Brodsky, P. Hoyer, Nucl. Phys. B **383**, 643 (1992); R. Vogt, S.J. Brodsky, Nucl. Phys. B **438**, 261 (1995); T. Gutierrez, R. Vogt, Nucl. Phys. B **539**, 189 (1999); R. Vogt, Z. Phys. C **71**, 475 (1996); G. Anzivino et al., Nuovo Cim. A **107**, 955 (1994); N. Armesto, C. Pajares, Yu.M. Shabelski, Preprint of Universidade de Santiago de Compostela, hep-ph/9506212, 1995; O.I. Piskounova, Nucl. Phys. Proc. Suppl. **50**, 179 (1996); G.H. Arakelyan, P.E. Volkovitsky, Z. Phys. A **353**, 87 (1995)
16. G.H. Arakelyan, Phys. Atom. Nucl. **61**, 1570 (1998)
17. V.A. Bednyakov, Mod. Phys. Lett. A **10**, 61 (1995)
18. A.K. Likhoded, S.R. Slabospitsky, Phys. Atom. Nucl. **60**, 981 (1997); **62**, 693 (1999)
19. E. Cuautle, G. Herrera, J. Magnin, Eur. Phys. J. C **2**, 473 (1998)
20. Yu.M. Shabelski, hep-ph/0011032
21. R.C. Hwa, Phys. Rev. D **51**, 85 (1995); K.P. Das, R.C. Hwa, Phys. Lett. B **68**, 459 (1977)
22. J. Dias de Deus, F.O. Duraes, Eur. Phys. J. C **13**, 647 (2000)
23. J.C. Anjos et al. (E691), Phys. Rev. Lett. **62**, 513 (1989); M.P. Alvarez et al. (NA14/2), Z. Phys. C **60**, 53 (1993); P.L. Frabetti et al. (E687), Phys. Lett. B **370**, 222 (1996)
24. E. Braaten, Yu Jia, T. Mehen, hep-ph/0111296
25. T. Tashiro, H. Noda, S. Nakariki, K. Ishii, K. Kinoshita, Eur. Phys. J. C **2**, 733 (1998)
26. H. Minakata, Phys. Rev. D **20**, 1656 (1979)
27. G. Cohen-Tannoudji, A. El Hassouni, J. Kalinowski, R. Peschanski, Phys. Rev. D **19**, 3397 (1979)
28. K. Kinoshita, H. Noda, T. Tashiro, Prog. Theor. Phys. **68**, 1699 (1982); **68**, 2086 (1982); T. Tashiro, H. Noda, K. Kinoshita, C. Iso, Z. Phys. C **35**, 21 (1987)
29. K. Kinoshita, H. Noda, T. Tashiro, J. Nagao, International Symposium on High Energy Nuclear Collisions and Quark Gluon Plasma, Kyoto 1991, edited by M. Biyajima, H. Enyo, T. Kunihiro, O. Miyamura (World Science, Singapore 1992), p. 245
30. K. Kinoshita, A. Minaka, Prog. Theor. Phys. **81**, 183 (1989)
31. L. Burakovsky, T. Goldman, Phys. Lett. B **434**, 251 (1998)
32. M. Aguilar-Benitez et al., Phys. Lett. B **169**, 157 (1996)
33. E.M. Aitala et al. (E791), Phys. Lett. B **411**, 230 (1997)